applied optics

Fast auto-focusing search algorithm for a high-speed and high-resolution camera based on the image histogram feature function

CHENZI GUO,[1,2] ZELONG MA,[1,*] XU GUO,[1,2] WENXIAN LI,[1,2] XINDA QI,[1] AND QINGLEI ZHAO[1]

[1]Changchun Institute of Optics, Fine Mechanics and Physics, Chinese Academy of Sciences, Changchun 130033, China
[2]University of Chinese Academy of Sciences, Beijing 100039, China
*Corresponding author: mazelong1985@126.com

Received 13 June 2018; revised 14 September 2018; accepted 1 October 2018; posted 1 October 2018 (Doc. ID 334958); published 24 October 2018

In this paper, we developed an auto-focus image quality evaluation function from the histogram feature function (HFF) of a high-speed camera. Based on this function, we then proposed a fast auto-focus search algorithm. We further demonstrated that the auto-focus image quality evaluation function we proposed requires fewer computational resources, while providing a more effective focusing area and more moderate sensitivity, compared to the traditional evaluation function. In contrast to the traditional climbing method, our proposed fast auto-focusing search algorithm also can spot the focus point in a shorter time, effectively reducing the round trips of the focusing motor and improving the focusing accuracy.

https://doi.org/10.1364/AO.57.000F44

1. INTRODUCTION

High-speed cameras have been extensively used in working environments where the focal length varies greatly, such as photoelectric theodolites. In such situations, the image plane of the target is difficult to maintain in the focal plane of the image sensor, owing to the drastic change of the distance between the fast-moving target and the camera. As a result, the camera continuously captures a large number of images, some of which are out of focus and short of necessary image details. Therefore, automatic focusing methods are introduced to solve the issue, including active focusing and passive focusing. The active focusing system is highly dependent on external devices since its target-to-camera distance is obtained via external measuring components, such as infrared rays, ultrasonic waves, or lasers. A passive focusing system [1], however, is much more desirable because it is less dependent on external devices. In a passive focusing system, the image defocus can be analyzed by the image sharpness evaluation function and adjustments are then performed according to search methods [2–4].

The current image sharpness evaluation function can be divided into three varieties: the threshold integration method [5,6], the threshold differential method [7,8], and band integration method [9–14]. The threshold integration method functions by integrating the pixels of the image before establishing an evaluation function based on the gray level change, such as information entropy. The threshold differential method extracts feature information by performing differential operations on the image, such as sum modulator, Brenner operator, Sobel gradient operator, and Laplacian gradient operator. The band integration method, such as FFT, DCT, and power spectrum (PS), uses the image's high-frequency part to evaluate its sharpness. Unfortunately, these three methods all have flaws that cannot be ignored: The threshold integration method offers less accuracy; the threshold differential method only allows for a small effective focusing range; and the band integration method requires too much calculation. To summarize, none of the aforementioned methods can meet the need for fast, wide-range focusing in high-speed, high-resolution cameras. Meanwhile, the present image-processing-based focusing search methods are of two general categories: one that identifies the focus point via searching, such as the function approaching method, Fibbonacci search method and climbing method; and the fast searching method [15–21] that can calculate the focus position by parallax, phase difference, and image dispersion circle, such as the dual camera parallax method, PDAF method, and defocusing depth method. The former method is inaccurate, slowly convergent, and possibly concussive around an extreme point. The latter method is inaccurate and restricted by the inherent characteristics of the high-speed camera. Therefore, none of the methods prove to be effective for auto-focusing high-speed cameras.

To address this issue, our paper begins with how a high-speed camera can be driven by passive focusing to accurately spot the focal point and provide better insight for subsequent eye and machine observation. Then an image sharpness evaluation function based on the image histogram eigenfunction is proposed, which has not only reduced the calculation amount, but also realized a large effective range and highly accurate image capture. Based on this evaluation function, a search method is designed for fast and wide-range focusing of high-speed and high-resolution cameras.

2. PRINCIPLE AND DESIGN OF ALGORITHM

In the passive focusing method, the focus adjustment effect mainly depends on the image sharpness evaluation function and the focus search method. For application to high-speed cameras, the image sharpness evaluation function is supposed to have not only great unimodality but also excellent real-time performance. Moreover, the focus search algorithm should also reduce the circling number to improve the real-time performance of search algorithms.

A. Image Sharpness Evaluation Function Based on the Histogram Feature Function

The gray histogram is a function of the image's gray value, which represents the statistical distribution of a image's gray values. Let the input image be $I(x, y)$, where there are x, y pixels; the gray level be L; and the grayscale histogram of $I(x, y)$ be $h(i)$ so that

$$h(i) = \sum_{x,y} C_i(x, y) \qquad (i = 0, \ldots, 2^L - 1; x, y \in N^+), \quad \textbf{(1)}$$

where

$$C_i(x, y) = \begin{cases} 1 & (I(x, y) = i) \\ 0 & (\text{otherwise}) \end{cases}. \quad \textbf{(2)}$$

Next, normalize the histogram so that

$$\text{norm}(i) = \frac{h(i)}{xy}, \quad \textbf{(3)}$$

$$\sum_i \text{norm}(i) = 1. \quad \textbf{(4)}$$

However, the gray histogram cannot be interpreted by machines; thus, the HFF is introduced as the probability density function when the luminance value is above the threshold (th) in the normalized image histogram. The sum of the mathematical expressions of HFF is

$$\text{HF(th)} = \sum_{i=\text{th}}^{2^L-1} \text{norm}(i) \qquad (\text{th} \in i = 0, \ldots, 2^L - 1). \quad \textbf{(5)}$$

Further, we established an image quality evaluation function H_diff based on the image histogram eigenfunction as given by

$$H\_\text{diff} = \text{MIN}\{|H\_\text{twice} - H\_\text{mean}|, \\ \times |H\_\text{mean} - H\_\text{half}|\}, \quad \textbf{(6)}$$

where H_mean, H_half, and H_twice are HFF function values when h is the function value of the average luminance value when th is the average luminance value, th is the HF function value when the average luminance value is half, and th is the HF function value when the luminance value is double. Through H_diff, we can not only filter the image sequence with great focusing effect but also preliminarily determine the defocus degree of a specific image. We divide the H_diff values into five levels—excellent, good, average, fair, and poor to evaluate the focusing search step length in the fast auto-focus search algorithm, as shown in Table 1.

Table 1. H_diff Value Distribution

Excellent	Good	Average	Fair	Poor
≤0.1	0.1–0.16	0.17–0.22	0.23–0.29	> 0.3

The HFF-based image quality evaluation function can evaluate the captured image of the camera in a relatively short time. This feature agrees with the other three image quality evaluation function indices (i.e., the focusing error, sensitivity, and effective area), as verified in subsequent experimental sections.

B. Fast Auto-Focus Search Algorithm

In the conventional auto-focusing search algorithm based on the hill-climbing method, the motor must search for multiple round trips in the vicinity of the peak, resulting in a long focusing time and the problem of defocusing accuracy caused by the motor's empty back phenomenon. These issues arise because the hill-climbing search algorithm requires multiple sampling of the focusing curve to determine the focus area. However, when a high-speed camera performs a task, because the frame rate is high, images of multiple frames may be acquired during each movement of the focus motor, and when the captured image is evaluated using a histogram feature function (HFF), it can be obtained in real time. The evaluation value of each frame of the image is obtained during the travel of the motor. In this manner, the image evaluation curve can be constructed using these image quality evaluation values obtained during the course of travel. Once it is determined that the search has crossed the position of the pseudo-focus, after the calculation, the motor can be directly driven to the position of the pseudo-focus.

As shown in Fig. 1, the fast auto-focusing algorithm records the H_diff value of the captured image at the initial position of the motor as H1, determines the initial search offset by the H_diff value level at which H1 is located, and then moves the value twice again to obtain the H2 and H3 values. Through these three values, the fast method first determines whether the search enters the main peak of the evaluation curve for the search direction and the slopes k1 and k2 formed by the three evaluation values of H1, H2, and H3. Once the search enters the main peak, the search step length is changed. For a fixed value, the slope is used to determine whether the search has crossed the peak. If the peak is exceeded, then the number of motor movements where the image quality evaluation maximum value frame number appears a number of times during the search, and the movement is performed twice. The number of frames included in the movement and the position information of the motor, after calculating the position of the quasi-focal point, are used to drive the motor to focus, and the formula to calculate the position of the quasi-focal point is represented by

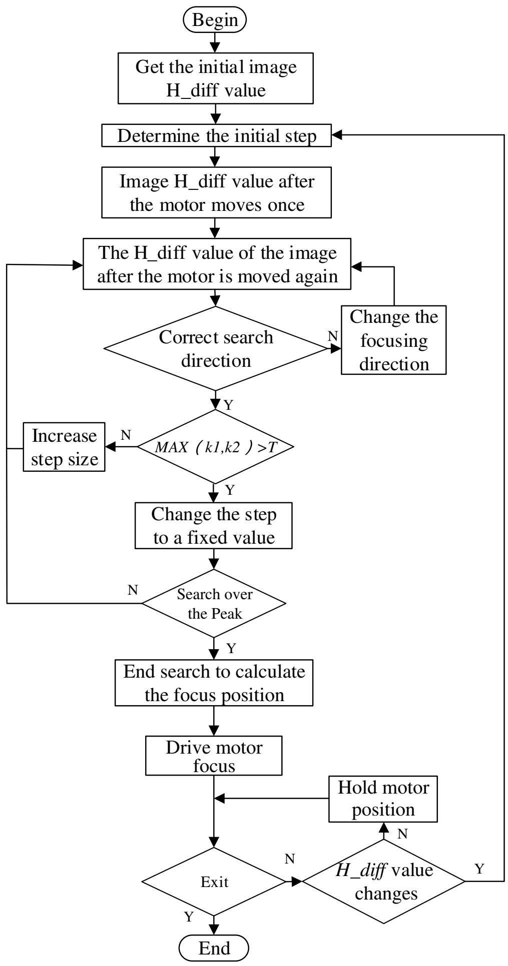

Fig. 1. Fast auto-focus search strategy flowchart.

$$S_{\max} = S_{\mathrm{Left}} + \left[\frac{S_{\mathrm{Right}} - S_{\mathrm{Left}} - 1}{F} \times F_{\max} \right], \quad (7)$$

where $S_{\max}$ is the quasi-focal position; S_{Left} and S_{Right} are the motor positions before and after the maximum number of movement times, respectively; F is the number of all frames included in the three movements; and $F_{\max}$ is the maximum value at the position in F. The calculated value is rounded and added to S_{Left} to drive the motor to focus.

3. EXPERIMENT

The experimental platform of this article includes two parts: high-speed camera and PC. The resolution, gray level, and working frame rate of the camera are 1024×1024, 200 frames/s, and 8-bit gray level, respectively. The configuration of the PC is an Intel I7-6700 eight-core processor with 8 GB memory running software written in VC++ language under Windows 7×64-bit system and compiled by Visual Studio 2010 software.

A. Focus Evaluation Function Experimental Results

Under the conditions of normal lighting, strong front lighting, and strong back lighting, three groups of images are used to evaluate our proposed evaluation function and existing evaluation functions. Each group contains 24 defocus images, as partly shown in Fig. 2.

This paper compares several representative image quality evaluation functions: information entropy function, Sobel operator, Laplacian operator, two-dimensional (2D) discrete Fourier transform, and 2D discrete cosine transform. The image in Fig. 2 was evaluated using the five functions mentioned above, since the sequence of images is arranged from the sharpest image to the least clear image, the ideal curve for all functions should be a monotone decreasing curve (i.e., the evaluation value should be maximum for the first image

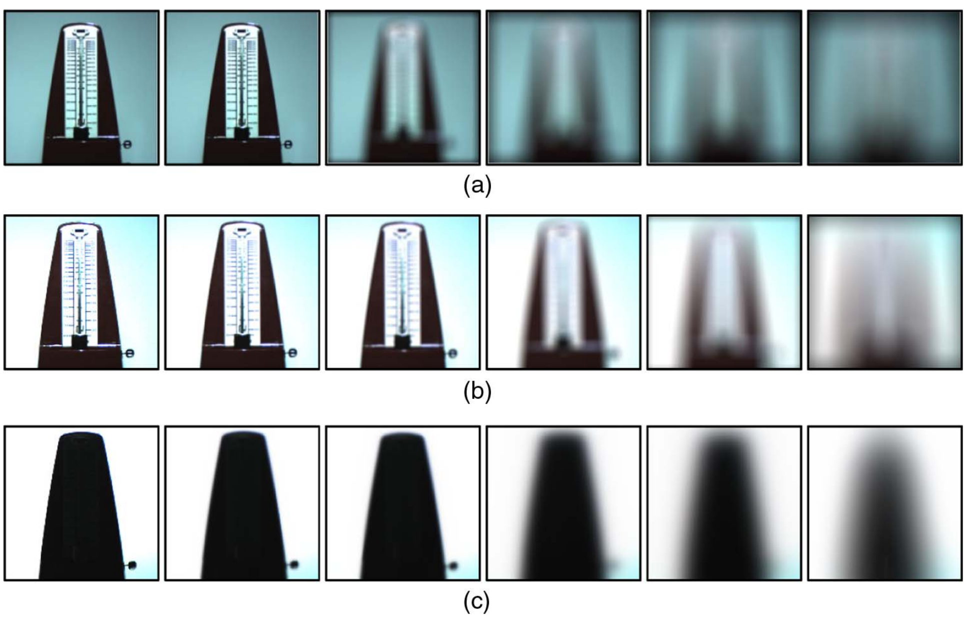

Fig. 2. Defocused image sequence partial image: (a) images under normal lighting; (b) images under strong front lighting; and (c) images under strong back lighting.

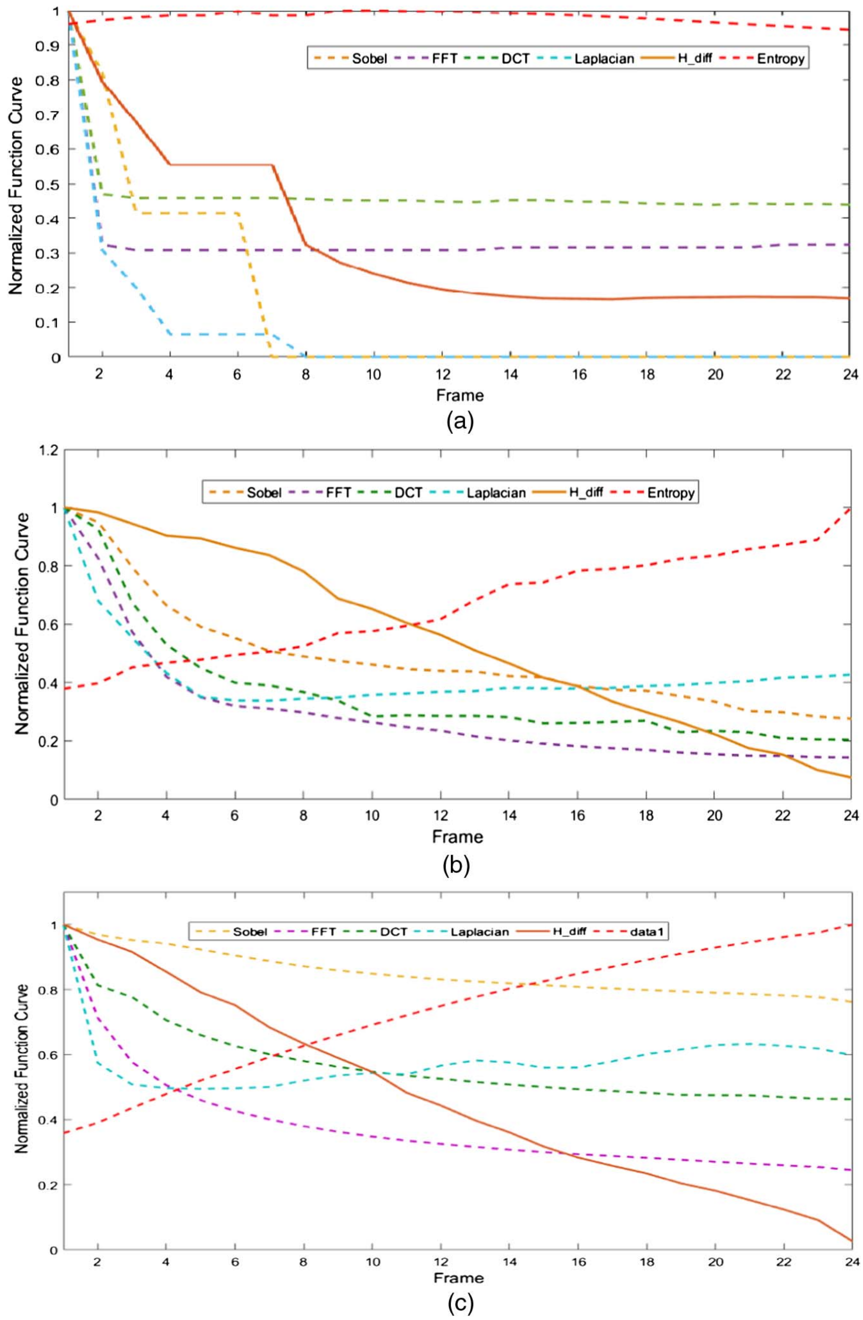

Fig. 3. Automatic focusing evaluation function comparison: (a) normal light condition; (b) strong front lighting; and (c) strong back lighting.

and then gradually reduced to the last image). To facilitate the observation, the obtained function curve is normalized, as shown in Fig. 3.

Further, we evaluated the performance of each auto-focus evaluation function from five perspectives:

(1) Error: The distance from the best imaging position to the peak position of the focus evaluation curve;

(2) Sensitivity: The sensitivity can indicate the sensitivity of the curve to the defocus of the image. High sensitivity indicates that the evaluation curve will decay rapidly when a small amount of defocus occurs. The mathematical expression of the sensitivity evaluation is

$$\text{Response} = \sum_{i=1}^{6} \frac{1}{|i| f(R+i)}, \qquad i \neq 0. \tag{8}$$

(3) Effective area: The effective area defines the number of consecutive images, whose absolute value of the image derivative is greater than a certain threshold in the continuous image quality evaluation function curve;

(4) Single pixel calculation amount: the number of additions and multiplications required by an image quality evaluation function to process a single pixel; and

(5) $1k \times 1k$ image calculation amount: The image quality evaluation function adds and multiplies the number of times required for processing the resolution of a $1k \times 1k$ image.

Table 2. Performance Evaluation of the Auto-Focusing Evaluation Function

		Entropy	Sobel	Laplacian	FFT	DCT	H_diff
Normal light condition	Error	9	0	0	0	0	0
	Sensitivity	0.3252	2.4534	12.7316	4.6351	3.1420	4.1420
	Effective area	24	7	4	2	2	14
Strong front lighting	Error	24	0	0	0	0	0
	Sensitivity	0	2.9615	3.9736	3.8722	3.3665	2.5548
	Effective area	24	24	5	24	24	24
Strong back lighting	Error	24	0	0	0	0	0
	Sensitivity	0	2.5322	3.7670	3.5965	2.9659	2.6543
	Effective area	24	24	4	24	24	24
Calculation consumption in all conditions	Single pixel calculation amount (sum/multiplication)	3/1	12/4	9/9	—	—	6/1
	$1k \times 1k$ image calculation amount (addition/multiplication)	$9k^2/k^2$	$144k^2/16k^2$	$81k^2/9k^2$	$40k^2/20k^2$	$17k^2+8k/27k^2+4k$	$6k^2/k^2$

As shown in Fig. 3 and Table 2, when the feature function based on the grayscale histogram is used as a focusing function, its sensitivity is comparable to the 2D Fourier transform, the effective area is relatively large in several evaluation functions, and the function, regardless of the computational requirements of a single pixel or the entire image, is lower than other functions. The focus adjusting effect still stands even when the background light varies dramatically. Such a function is an image quality evaluation function suitable for high-speed camera automatic focus detection and focusing.

B. Automatic Focus Search Experiment Results

To verify the effectiveness of the proposed auto-focus search algorithm, a fast auto-focus search algorithm was compared with the traditional hill-climbing algorithm. The experimental high-speed camera was equipped with a zoom lens with a focusing range of 5.8–69.6 mm (optical lens). The focal length range corresponds to stepper motor steps from 31 to 160 steps with a maximum stroke of 130 steps. The focal depth of the lens is determined to be approximately two steps, which is 1/65 of the entire focusing stroke and is the dichotomy of focal depth. One starts focusing as the course focusing start step (i.e., the basic step is a single step length of the stepping motor). After the measurement, the standard focal position corresponds to the position of the stepping motor after 103 steps. The image quality evaluation functions of the hill-climbing method and the fast automatic focusing search algorithm are HF functions. The obtained experimental data are shown in Table 3.

The experimental results show that the quasi-focal position obtained by the fast search method is the same as the traditional search algorithm. However, after the fast auto-focus search method is applied, the motor only changes the direction once and the quasi-focal position is found. Compared with the traditional autofocus method, which takes 22 moves to complete the focus, the fast algorithm requires only nine moves to complete the focus, greatly reducing the auto-focus time of high-speed cameras.

Table 3. Experimental Results

	Motor Movement Times	Motor Change Direction Times	Error (Steps)
Traditional hill-climbing method	22	3	0
Fast auto-focus search algorithm	9	1	0

4. CONCLUSION

In this paper, an auto-focus image evaluation function based on the image histogram feature function was proposed to feed the needs of high-speed cameras and camera characteristics. On its basis, a fast auto-focusing algorithm was further proposed. Compared to the previous evaluation functions, our proposed function is advantageous in calculation speed, focusing precision, and effective focusing range. Experiments show that this function is satisfiable when applied to a wide-range, high-speed camera. Our proposed algorithm also proves to be faster, but as accurate, in focusing, which enables the high-speed camera to capture clearer images.

Funding. National Natural Science Foundation of China (NSFC)61742501

Acknowledgment. The authors declare that no conflicts of interest exist in/are related to this article.

REFERENCES

1. M. Subbarao and G. Surya, "Depth from defocus: a spatial domain approach," Int. J. Comput. Vis. **13**, 271–294 (1994).
2. S. Y. Park and J. Moon, "Image-based calibration of spatial domain depth-from-defocus and application to automatic focus tracking," in *Asian Conference on Computer Vision*, P. J. Narayanan, S. K. Nayar, and H. Y. Shum, eds. (Springer, 2006), pp. 754–763.
3. C. F. J. Kuo and C. H. Chiu, "Improved auto-focus search algorithms for CMOS image-sensing module," J. Inf. Sci. Eng. **27**, 1377–1393 (2011).
4. M. Moscaritolo, H. Jampel, F. Knezevich, and R. Zeimer, "An image based auto-focusing algorithm for digital fundus photography," IEEE Trans. Med. Imaging **28**, 1703–1707 (2009).
5. Y. Wang, H. Feng, Z. Xu, Q. Li, and Y. Chen, "Autofocus evaluation function based on saturate pixels removing," Acta Opt. Sin. **36**, 1210001 (2016).
6. M. T. Rahman, *Real-Time Face-Priority Auto-Focus and Adaptive Auto-Exposure for Digital and Cell-Phone Cameras* (The University of Texas, 2011).

7. Y. Yi, A. Besma, D. Narjes, and A. Mongi, "Evaluation of sharpness measures and search algorithms for the auto focusing of high-magnification images," Proc. SPIE **6246**, 62460G (2006).
8. Z. Ling, "Adaptive autofocusing: a closed-loop perspective," J. Opt. Soc. Am. A **22**, 625–635 (2005)
9. X. Sha, W. Li, X. Lv, J. Lv, and Z. Li, "Research on auto-focusing technology for micro vision system," Optik **142**, 226–233 (2017).
10. Y. Wang, H. Feng, Z. Xu, Q. Li, and Y. Chen, "An adjustable coverage range autofocus evaluation function using gradient operator with variable frequency," Inf. Laser Eng. **45**, 1028001 (2016).
11. B. K. Park, S.-S. Kim, D.-S. Chung, S. Lee, and C. Y. Kim, "Fast and accurate auto focusing algorithm based on two defocused images using discrete cosine transform," Proc. SPIE **6817**, 68170D (2008).
12. G. Jiang, W. Yi, M. Yu, and M. Yang, "Digital autofocusing method based on contourlet transform," Optoelectron. Lett. **3**, 381–384 (2007).
13. M. A. Bueno-Ibarra, J. Alvarez-Borrego, L. Acho, and M. C. Chavez-Sanchez, "Fast autofocus algorithm for automated microscopes," Opt. Eng. **44**, 063601 (2005).
14. G. J. Wang, *Research on Auto-Focusing Method of Photoelectric Measurement Equipment Based on Image Processing* (University of Chinese Academy of Sciences, 2016).
15. H. Ou, Y. Wu, E. Y. Lam, and B.-Z. Wang, "New autofocus and reconstruction method based on a connected domain," Opt. Lett. **43**, 2201–2203 (2018).
16. Y. Zhang, H. Wang, Y. Wu, M. Tamamitsu, and A. Ozcan, "Edge sparsity criterion for robust holographic autofocusing," Opt. Lett. **42**, 3824–3827 (2017).
17. S. Jiao, P. W. M. Tsang, T.-C. Poon, J.-P. Liu, W. Zou, and X. Li, "Enhanced autofocusing in optical scanning holography based on hologram decomposition," IEEE Trans Ind. Inf. **13**, 2455–2463 (2017).
18. T. Pitkäaho, A. Manninen, and T. J. Naughton, "Performance of autofocus capability of deep convolutional neural networks in digital holographic microscopy," in *Digital Holography and Three-Dimensional Imaging* (Optical Society of America, 2017), paper W2A.5
19. X. Lin, J. Suo, G. Wetzstein, Q. Dai, and R. Raskar, "Coded focal stack photography," in *IEEE International Conference on Computational Photography (ICCP)* (IEEE, 2013), pp. 1–9.
20. X. Lin, J. Wu, G. Zheng, and Q. Dai, "Camera array based light field microscopy," Biomed. Opt. Express **6**, 3179–3189 (2015).
21. R. Ng, M. Levoy, M. Brédif, G. Duval, M. Horowitz, and P. Hanrahan, "Light field photography with a hand-held plenoptic camera," Stanford Tech. Report CTSR 2005-02 (2005), pp. 1–11.